Photochemical & Photobiological Sciences

PAPER

View Article Online
View Journal | View Issue

Cite this: *Photochem. Photobiol. Sci.*, 2016, **15**, 889

Experimental evidence of incomplete fluorescence quenching of pyrene bound to humic substances: implications for K_{OC} measurements†

E. A. Shirshin,*[a] G. S. Budylin,[a] N. Yu. Grechischeva,[b] V. V. Fadeev[a] and I. V. Perminova[c]

Fluorescence quenching (FQ) is extensively used for quantitative assessment of partition coefficients (K_{OC}) of polycyclic aromatic hydrocarbons (PAHs) to natural organic materials – humic substances (HS). The presence of bound PAHs with incompletely quenched fluorescence would lead to underestimation of the K_{OC} values measured by this technique. The goal of this work was to prove the validity of this assumption using an original experimental setup, which implied FQ measurements upon excitation into two distinct vibronically coupled electronic states. Pyrene was used as a fluorescent probe, and aquatic fulvic acid (SRFA) and leonardite humic acid (CHP) were used as the humic materials with low and high binding affinity for pyrene, respectively. Excitation of pyrene into the forbidden (S_0–S_1) and allowed (S_0–S_2) electronic states yielded two pairs of nonidentical FQ curves. This was indicative of incomplete quenching of the bound pyrene, and the divergence of the two FQ curves was much more pronounced for CHP as compared to SRFA. The two component model of fluorescence response formation was proposed to estimate the K_{OC} values from the data obtained. The resulting pyrene K_{OC} value for CHP (220 ± 20) g L^{-1} was a factor 3 higher compared to the K_{OC} value determined with the use of the Stern–Volmer formalism (68 ± 2) g L^{-1}. At the same time for aquatic FA the difference in FQ curves was almost negligible, which enables the use of the Stern–Volmer formalism for weakly interacting HS and PAHs.

Received 21st February 2016,
Accepted 23rd May 2016

DOI: 10.1039/c6pp00052e

www.rsc.org/pps

Introduction

Interactions of polycyclic aromatic hydrocarbons (PAHs) with natural organic matrices, *e.g.* humic substances (HS), are of serious environmental concern due to the multiple adverse effects of these hydrophobic contaminants on living organisms.[1–3] Binding to HS causes an increase in mobility and a change in the bioavailability and toxicity of PAHs.[4–6] To quantify and prognosticate these effects, partition coefficients (K_{OC}) of PAHs to HS are used for geochemical and ecotoxicological modeling. To determine K_{OC}, fluorescence quenching (FQ) of PAHs by HS is widely used.[6–14] Upon determining K_{OC} from FQ curves, it is commonly assumed that PAHs bound to HS are completely quenched.[7] This enables the use of the Stern–Volmer formalism. Still, indications of incomplete quenching of PAHs in the presence of HS were obtained.[8,15–24] A significant change in the relative intensities of vibronic peaks in pyrene fluorescence in the presence of HS was revealed using measurements at room[16,18–22] and ultralow[17] temperatures. To explain the observed results, the presence of weakly bound pyrene with nonzero quantum yield was suggested.[17] A similar suggestion was made to accommodate results of time-resolved fluorescence measurements of pyrene bound to dissolved HS: its fluorescence lifetime increased compared to free pyrene molecules indicating the presence of different species of pyrene in HS solutions.[24]

Given that pyrene interacts with HS mostly *via* hydrophobic binding, incomplete quenching looks rather feasible.[25,26] Still, quantitative assessments of this phenomenon are missing.

In this work, we propose an original experimental setup to acquire FQ measurements, which could enable observation of pyrene bound to HS. For this purpose we measured FQ curves of pyrene upon its excitation into two vibronically coupled states (the forbidden S_1 state and the allowed S_2 state). In the case of static quenching, both FQ curves should be identical. A difference between the FQ curves is indicative of the presence of pyrene–HS complexes with a nonzero fluorescence cross

[a]*Department of Physics, Lomonosov Moscow State University, Leninskie Gory 1-2, 119991 Moscow, Russia. E-mail: shirshin@lid.phys.msu.ru; Fax: +7(495)9391653; Tel: +7(495)9391653*
[b]*Russian State University for Oil and Gas named after I.M. Gubkin, Leninskiy Prosp. 65-1, 119991 Moscow, Russia*
[c]*Department of Chemistry, Lomonosov Moscow State University, Leninskie gory 1-3, 119991 Moscow, Russia*

†Electronic supplementary information (ESI) available: Detailed description of the protocol of fluorescence measurements. See DOI: 10.1039/c6pp00052e

section. To reveal this phenomenon, we used two HS samples with a low and high binding affinity for pyrene.

Backgrounds

Fluorescence characteristics of the pyrene–HS system: the two-component model of the fluorescent response formation

Interactions in the system containing pyrene (Py) and HS can be schematically represented by the following reaction:

$$\mathrm{Py} + \mathrm{HS} \leftrightarrow \mathrm{PyHS} \quad (1)$$

The corresponding partition coefficient (K_{OC}) is:

$$K_{OC} = \frac{[\mathrm{PyHS}]}{[\mathrm{Py}][\mathrm{HS}]} \quad (2)$$

where [PyHS] is the equilibrium concentration of pyrene bound to HS, [Py] and [HS] are the equilibrium concentrations of free pyrene and HS species, respectively. If the total concentration of HS (C_{HS}) substantially exceeds [HS], the latter might be set equal to C_{HS}. Considering that [Py] + [PyHS] = C_{Py}, where C_{Py} is the total concentration of pyrene in solution, the concentration of free pyrene can be expressed from (2) as

$$[\mathrm{Py}] = \frac{C_{Py}}{1 + K_{OC}C_{HS}}. \quad (3)$$

If fluorescence of the bound pyrene is completely quenched (static quenching), then residual fluorescence (F) in the system can be described as:

$$F \sim \Sigma \cdot I_0 \cdot [\mathrm{Py}] = \sigma \cdot \eta \cdot I_0 \cdot [\mathrm{Py}] \quad (4)$$

where Σ stands for the fluorescence cross-section, which is a product of the absorption cross-section σ and the fluorescence quantum yield η, and I_0 is the excitation intensity. Using eqn (3) and (4), the Stern–Volmer equation can be obtained:

$$\frac{F_0}{F} = \frac{\Sigma \cdot I_0 \cdot C_{Py}}{\Sigma \cdot I_0 \cdot [\mathrm{Py}]} = 1 + K_{OC}C_{HS} \quad (5)$$

where F_0 is the fluorescence intensity of pyrene in the absence of HS.

If photophysical parameters of the bound pyrene are different from those of free pyrene, and its fluorescence quantum yield is nonzero, then from eqn (3) and (4) the following quenching equation can be obtained:[13,14]

$$F_0/F = \frac{\Sigma_F C_{Py}}{\Sigma_F[\mathrm{Py}] + \Sigma_B[\mathrm{PyHS}]} = \frac{1 + K_{OC}C_{HS}}{1 + R \cdot K_{OC}C_{HS}} \quad (6)$$

where $R = \Sigma_B/\Sigma_F$, Σ_B and Σ_F stand for the fluorescence cross-sections of bound and free pyrene species, respectively. This equation becomes identical to eqn (5) in the case of nonfluorescent complexes ($R = 0$). Hereby, the two-component model of pyrene fluorescence leads to dependence of FQ curves on the ratio of the photophysical parameters, which determines the fluorescence efficiency of free and bound pyrene.

To detect the contribution of the bound pyrene with nonzero fluorescence quantum yield we exploited the fact that the Stern–Volmer eqn (5) does not contain the photophysical parameters of pyrene fluorescence (*e.g.*, σ, η). It means that in the case of static quenching it should not depend on the excitation wavelength. Then, if a difference between the FQ curves is detected upon excitation of pyrene into two distinct electronic states, this can serve as an experimental proof of a fluorescent component other than free pyrene. To justify the validity of this approach, let us consider the processes, which underlie pyrene fluorescence when it is excited into two different electronic states.

Photophysical processes in pyrene upon its excitation into the S_1 and S_2 electronic states

A simplified electronic structure of the pyrene molecule is presented in Fig. 1. The $S_0 \rightarrow S_1$ transition is nominally forbidden, while the $S_0 \rightarrow S_2$ transition is allowed.[27] The S_1 and S_2 singlet excited states are closely separated with the energy gap between them, $\Delta E_{12} \approx 2700\ \mathrm{cm}^{-1}$, which is comparable to the energy of one pyrene vibrational mode. As a result, vibronic coupling between the S_1 and S_2 electronic states leads to an intensity borrowing effect, which is manifested as an enhancement of the weak $S_0 \rightarrow S_1$ transition intensity by vibrational coupling to the neighboring S_2 state due to oscillator strength exchange.[28]

Given that any change in the pyrene microenvironment polarity leads to alteration in the intensity borrowing degree and in mixing between its electronic states,[29–31] it will be manifested in opposite changes in extinction coefficients of

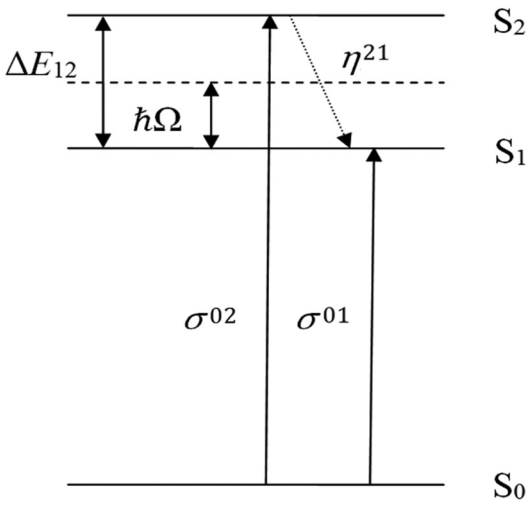

Fig. 1 Simplified electronic structure of the pyrene molecule. Two-sided arrows demonstrate the energy scales: $\hbar\Omega$ is the energy of the oscillatory mode for pyrene, and ΔE_{12} is the difference between the S_2 and S_1 electronic states. For the closely-lying S_1 and S_2 states vibronic coupling takes place, which influences oscillator strength of the corresponding transitions. One-sided arrows indicate the following transitions: $S_0 \rightarrow S_1$ and $S_0 \rightarrow S_2$ absorption with σ_{01}, σ_{02} cross-sections and $S_2 \rightarrow S_1$ conversion characterized by the probability η_{21}.

the $S_0 \rightarrow S_2$ and $S_0 \rightarrow S_1$ transitions. This is because an increase in the intensity of $S_0 \rightarrow S_1$ transition due to oscillator strength exchange with the $S_0 \rightarrow S_2$ transition brings about a decrease in the transition cross-sections σ^{01} and σ^{02}. Indeed, the extinction coefficient of the $S_0 \rightarrow S_2$ transition increases along with a decrease in the solvent polarity.[31,32] At the same time, a lower value of the absorption cross-section σ^{01} is observed in the less polar environments. For instance, a factor of four decrease was observed in the σ_{01} value upon replacing acetonitrile with cyclohexane.[33] The same trend is observed for other aromatic hydrocarbons with a high degree of symmetry, which is indicative of the enhancement of weakly allowed vibronic transitions in polar solvents.[34]

Hence, pyrene excitation into the S_1 and S_2 electronic states will be accompanied by a change in the ratio of the corresponding fluorescence intensities F^{01}/F^{02}, which are connected to the values of σ^{01} and σ^{02}. While the polarity of the pyrene microenvironment is known to decrease upon binding to HS as compared to water,[15,16,19,22,24] we have deduced the following changes in the σ^{01} and σ^{02} values for free and bound pyrene species:

$$R^{01} = \frac{\Sigma_B{}^{01}}{\Sigma_F{}^{01}} = \frac{\sigma_B{}^{01}\eta_B}{\sigma_F{}^{01}\eta_F}, \quad (7a)$$

$$R^{02} = \frac{\Sigma_B{}^{02}}{\Sigma_F{}^{02}} = \frac{\sigma_B{}^{02}\eta_B{}^{21}\eta_B}{\sigma_F{}^{02}\eta_F{}^{21}\eta_F} = \frac{\sigma_B{}^{02}\eta_B}{\sigma_F{}^{02}\eta_F}, \quad (7b)$$

where the indexes "0i" stand for the $S_0 \rightarrow S_i$ excitation, the quantum yield of the $S_2 \rightarrow S_1$ transition is assumed to be unity ($\eta^{21} = 1$), and in both cases fluorescence emission results from the $S_1 \rightarrow S_0$ transition.

According to the suggested hypothesis, the $S_0 \rightarrow S_1$ absorption cross-section of the bound pyrene species $\sigma_B{}^{01}$ should be lower than that of the free pyrene species $\sigma_F{}^{01}$. This is because the pyrene incorporated into the HS matrix has a less polar microenvironment compared to water.[15,16,19,22,24] The same should be true for the $\sigma_B{}^{02}$ and $\sigma_F{}^{02}$ values, which should change in the opposite direction. As a result, fluorescence quenching in the pyrene–HS system upon $S_0 \rightarrow S_1$ excitation should be more pronounced compared to $S_0 \rightarrow S_2$ excitation.

This hypothesis can be formalized using the following inequality:

$$\frac{\sigma_B{}^{01}}{\sigma_F{}^{01}} < \frac{\sigma_B{}^{02}}{\sigma_F{}^{02}}, \quad (8)$$

which can be further combined with eqn (7):

$$R^{01}/R^{02} < 1 \quad (9)$$

Hence, the dissimilarity between the two FQ curves obtained upon excitation with different wavelengths is a strong indication of the nonzero quantum yield of the bound pyrene species. Moreover, the inequality (9) should hold for the parameters R^{01} and R^{02} measured at the $S_0 \rightarrow S_1$ and $S_0 \rightarrow S_2$ excitations, respectively. This suggestion was experimentally verified in this work.

Experimental

Reagents and chemicals

Humic materials. A standard sample of aquatic fulvic acids of the International Humic Substances Society (IHSS) (the Suwannee River fulvic acid, SRFA), and a sample of the leonardite humic acids (CHP), isolated from commercially available potassium humate, were used in this study.[35] Elemental analyses (C, H, N) were conducted using a Vario EL analyzer. The H/C and O/C atomic ratios were calculated as indicators of saturation degree and polarity of HS, respectively.

The distribution of carbon among major structural fragments was determined using ^{13}C NMR spectroscopy.[36,37] The samples were prepared for ^{13}C NMR studies by dissolving a weight of HS (50 mg) in 0.6 mL of 0.3 M NaOD/D_2O. The following assignments were made (in ppm):[36] 5 to 50—aliphatic C atoms (C_{Alk}), 50 to 108—aliphatic *O*-substituted C atoms (C_{Alk-O}), 108 to 145—aromatic C atoms (C_{Ar}), 145 to 165—aromatic *O*-substituted C atoms (C_{Ar-O}), 165 to 187—C atoms of carboxyl and ester groups ($C_{COO-H,R}$), 187 to 220—ketone groups ($C_{C=O}$). The corresponding data are summarized in Table 1.

Pyrene was purchased from Sigma-Aldrich 99% pure (Germany) and used as is. MilliQ-water and acetonitrile (spectrophotometric grade, ≥99.5%) were used for sample preparations.

Sample preparation for optical spectroscopy measurements

In the case of SRFA, the stock solution of 500 mg L^{-1} was prepared by dissolution of a solid sample in Milli-Q water. In the case of CHP, the solid sample was firstly soaked in few microliters of 3 M NaOH, and then diluted to a concentration of 500 mg L^{-1} using MilliQ-water. Pyrene aqueous solutions were prepared by spiking 1 L of MilliQ-water with 100 μL of pyrene stock solution in acetonitrile (400 mg L^{-1}) to make 40 μg L^{-1}. For fluorescence measurements, 3 mL of pyrene work solution were titrated with aliquots (5 μl) of HS stock solution to reach concentrations of HS from 0 up to 10 mg L^{-1}. pH was 5.8.

For fluorescence and absorption measurements the pyrene concentration was set to 0.8 mg L^{-1}.

Table 1 Characteristics of the HS samples used in this study

	Atomic ratios		Carbon distribution among major structural groups, % of the total C					
HS sample	H/C	O/C	C_{Alk}	C_{AlkO}	C_{Ar}	C_{ArO}	C_{COO}	$C_{C=O}$
SRFA	1.08	0.62	20	20	22	11	20	7
CHP	0.84	0.38	15	7	47	12	13	5

Fluorescence and absorption measurements

Fluorescence spectra were obtained using a FluoroMax-4 (Horiba Jobin Yvon) spectrofluorometer. For the $S_0 \rightarrow S_1$ pyrene excitation, the excitation wavelength (λ_{ex}) was 364 nm, excitation and emission slit widths were 5 and 1 nm, respectively, fluorescence emission was collected in the range from 369 to 600 nm. For the $S_0 \rightarrow S_2$ excitation, λ_{ex} was 334 nm, both slit widths were 1 nm, fluorescence emission was collected in the range from 350 to 600 nm. More details on experimental conditions are given in the ESI.†

Absorption spectra were obtained using the Lambda-25 (Perkin-Elmer) spectrophotometer in the 200–700 nm spectral region.

Fluorescence data treatment

The inner filter effect was accounted for using the corresponding absorption spectra.[7] All FQ curves for the forbidden $S_0 \rightarrow S_1$ transition were corrected for HS fluorescence by subtraction of the HS signal. The constant shape of the HS fluorescence band was assumed over all concentrations used, and the following discrepancy was minimized:

$$\chi^2 = \sum_i \left(S(\lambda_i) - \alpha \cdot S_{Py}(\lambda_i) - \beta \cdot S_{HS}(\lambda_i) - S_{H_2O}(\lambda_i)\right)^2, \qquad (10)$$

where $S(\lambda)$ is the spectrum of the sample under investigation, $S_{Py}(\lambda)$ is the spectral band shape of aqueous pyrene solution in the absence of HS, $S_{HS}(\lambda)$ is the fluorescence spectrum of the aqueous HS solution, $S_{H_2O}(\lambda)$ is the spectrum of Raman scattering of water molecules, and α and β are the coefficients, which characterize the contribution of pyrene and HS to the overall fluorescence.

As a result of this spectral decomposition, the coefficients α and β were obtained for different HS concentrations. The dependence of β on a number of aliquots added to the pyrene working solution was used to control the HS concentration in experimental solutions. Hence, for the $S_0 \rightarrow S_1$ transition the dependence of α on the HS concentration was used to obtain FQ curves: $\alpha([HS]) = F/F_0([HS])$, and to obtain FQ curves for the excitation into the $S_0 \rightarrow S_2$ allowed transition, integral fluorescence intensity in the range of 369–400 nm was used.

Fitting of fluorescence quenching curves either to the Stern–Volmer equation or to eqn (6) was performed with OriginPro 2015 using the Levenberg–Marquardt algorithm with instrumental weighting.

Results and discussion

Fluorescence quenching of pyrene bound to HS upon excitation into the S_1 and S_2 electronic states

Two humic materials were used in our studies: the aquatic fulvic acid (SRFA) with a high content of oxidized polar moieties, and the leonardite humic acid (CHP) with a high content of poorly-oxidized aromatic and aliphatic moieties (see Table 1). These humic materials differed greatly in binding affinity for pyrene,[38] which was low for SRFA and high – for CHP.

FQ curves were measured for both the humic materials at excitation into the S_1 and S_2 states of pyrene. We suggested that if the registered FQ curves differ from each other, this might be indicative of the nonzero quantum yield of the HS-bound pyrene (see eqn (2)).

Pyrene fluorescence spectra in the presence of 0, 5, and 10 mg L^{-1} of SRFA and CHP are presented in Fig. 2. Excitation into the allowed $S_0 \rightarrow S_2$ transition yielded strong pyrene fluorescence (Fig. 2A and C): HS fluorescence background could be neglected upon calculating fluorescence quenching. Excitation into the forbidden $S_0 \rightarrow S_1$ transition yielded a much lower intensity of pyrene fluorescence, which became comparable to HS (Fig. 2B and D). The latter implies decomposition of the spectra to obtain FQ curves. Water Raman scattering (at *ca.* 420 nm) can be clearly observed in Fig. 2B, while it is negligible in the case of S_0–S_2 excitation (Fig. 2A and C). A difference in pyrene fluorescence intensities at these two excitation regimes exceeds two orders of magnitude. The shape of pyrene fluorescence spectra in the absence of HS was identical for both the excitation wavelengths used in our study.

Fig. 3 represents the results of six independent measurements of FQ curves for SRFA and CHP. The amplitude of pyrene fluorescence quenching in the case of CHP is much larger as compared to SRFA. These results agree with our previous data on the significant correlation between HS aromaticity and PAH binding constants.[38,39] CHP contains a condensed aromatic core, while SRFA is much poorer in aromatic carbon (Table 1).

Another important observation is that fluorescence quenching at the $S_0 \rightarrow S_1$ excitation is more pronounced as compared to the $S_0 \rightarrow S_2$ excitation. Hence, the obtained FQ curves are not identical and the observed difference between $(F_0/F)^{01}$ and $(F_0/F)^{02}$ curves provides experimental evidence of the nonzero fluorescence quantum yield of the bound pyrene.

This can be explained by the lower σ^{01} and the higher σ^{02} absorption cross-section values for the bound pyrene as compared to free pyrene, which is in agreement with eqn (9). Pyrene bound to HS has a less polar microenvironment which results in the opposite changes in absorption cross-sections for the $S_0 \rightarrow S_1$ and $S_0 \rightarrow S_2$ transitions for free and bound pyrene. The inner filter effect cannot explain these results: it would lead to an opposite trend ($(F_0/F)^{01} < (F_0/F)^{02}$), while HS absorption is higher at the smaller wavelengths.

The divergence of FQ curves obtained at pyrene excitation into two distinct electronic states (S_1 and S_2) has an important implication for determination of the binding constants using the Stern–Volmer formalism.[1] To demonstrate this, we determined the K_{OC} value from both the FQ curves, obtained at $S_0 \rightarrow S_1$ and $S_0 \rightarrow S_2$ excitations using eqn (5), which does not take into account the fluorescence impact of bound pyrene (see Fig. S4 in the ESI†). The obtained results, presented in Table 2, were in agreement with the literature data.[40]

The obtained K_{OC} values were a factor of 2.1 and 1.4 larger in the case of CHP and SRFA, respectively. This was a result of

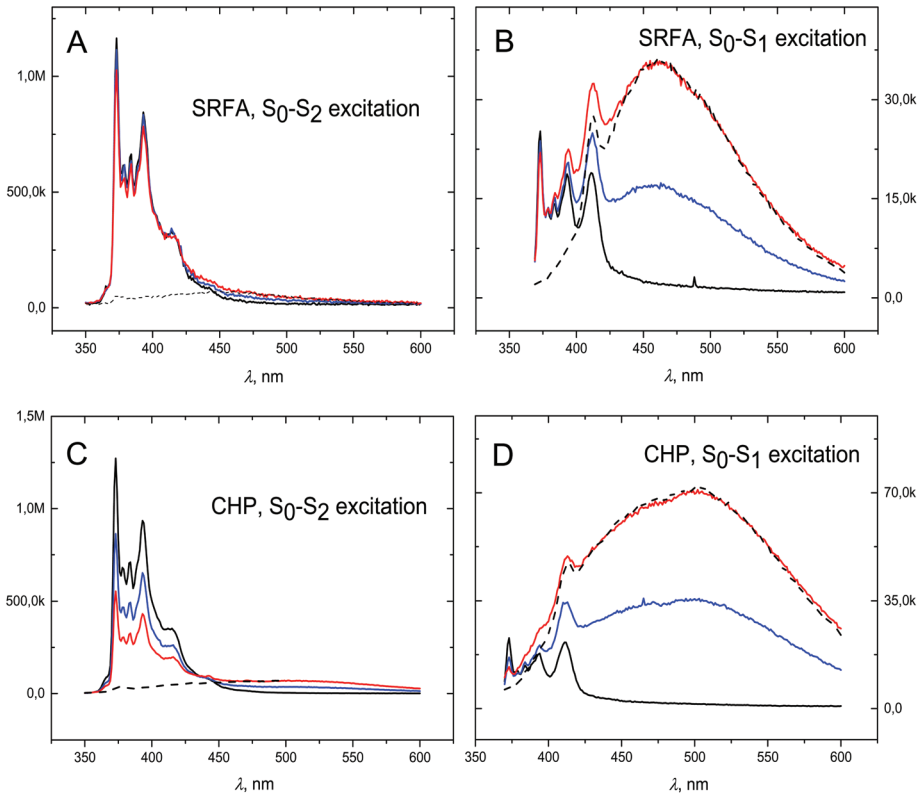

Fig. 2 The fluorescence spectra for aqueous solution of pyrene in the presence of different concentrations of SRFA and CHP (in mg L^{-1}): 0 (black curve), 5 (blue curve) and 10 (red curve). The spectra were obtained for the two excitation wavelengths: (A) and (C) the $S_0 \rightarrow S_2$ excitation (λ_{exc} = 334 nm) for SRFA and CHP: and (B) and (D) $S_0 \rightarrow S_1$ excitation (λ_{exc} = 364 nm) for SRFA and CHP. The black dashed curves correspond to the 10 mg L^{-1} HS fluorescence. The spectra are corrected for the inner filter effect.

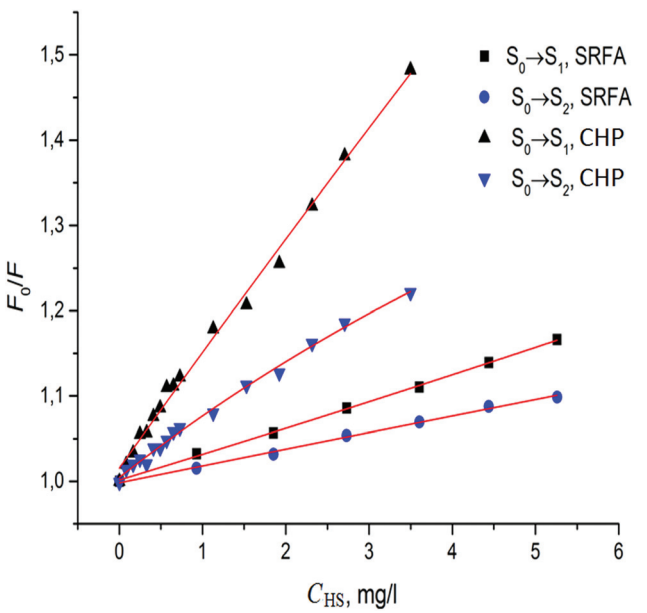

Fig. 3 Stern–Volmer plots for pyrene fluorescence quenching in the presence of two structurally different humic materials: aquatic fulvic acid (SRFA) and leonardite humic acid (CHP). The blue points are for the $S_0 \rightarrow S_2$ excitation (λ_{exc} = 334 nm), and the black ones are for the $S_0 \rightarrow S_1$ excitation (λ_{exc} = 364 nm). The value F was calculated as described in the Fluorescence data treatment section.

Table 2 The pyrene K_{OC} values determined under assumption of complete (eqn (5)) and incomplete (eqn (6)) FQ by HS

HS sample	Excitation	K_{OC}, L g^{-1} (eqn (5))	K_{OC}, L g^{-1} (eqn (6))
CHP	$S_0 \rightarrow S_1$	141 ± 3	220 ± 20
	$S_0 \rightarrow S_2$	68 ± 2	
SRFA	$S_0 \rightarrow S_1$	38.4 ± 0.6	n/d
	$S_0 \rightarrow S_2$	27.7 ± 0.8	

less quenching of the bound pyrene in the case of the $(F_0/F)^{02}$ curves as compared to the $S_0 \rightarrow S_1$ excitation. The difference in the K_{OC} values was more pronounced for CHP, which had a higher affinity for binding to pyrene.

Both the Stern–Volmer plots for CHP were further fitted to eqn (6), which takes into account the fluorescence impact of bound pyrene. This was not meaningful for SRFA, because the corresponding FQ curves yielded almost straight lines rendering determination of nonlinear parameters R impossible (see eqn (6)). Under the assumption that the K_{OC} values for both excitation wavelengths are equal, the R values accounted for: $R^{01} = 0.26 \pm 0.05$ and $R^{02} = 0.59 \pm 0.03$, which are in agreement with eqn (10). The K_{OC} value determined for CHP using eqn (6) was 220 ± 20 L g^{-1}, which is a factor of three larger as com-

pared to the K_{oc}^{02} value determined using the Stern Volmer formalism for static quenching.

Conclusions

The obtained results clearly demonstrate the substantial contribution of the bound pyrene in the measured fluorescence of the HS–Pyrene system which leads to underestimation of the K_{oc} value measured with the use of the FQ technique. Of particular importance is that this effect is proportional to the binding affinity of HS to pyrene reaching its highest contribution for the most hydrophobic and aromatic-rich HS capable of the strongest binding to PAHs. Hence, particular caution should be exercised when measuring FQ values of K_{oc} for these humic samples.

Acknowledgements

The authors would like to acknowledge the financial support of the Russian Foundation for Basic Research (grant no 15-05-09284). This work was partially supported by the Russian Science Foundation, project no 16-14-00167 (isolation and characterization of the humic materials).

References

1 I. C. Nisbet and P. K. LaGoy, Toxic equivalency factors (TEFs) for polycyclic aromatic hydrocarbons (PAHs), *Regul. Toxicol. Pharmacol.*, 1992, **16**, 290–300.
2 J. R. Almeida, C. Gravato and L. Guilhermino, Challenges in assessing the toxic effects of polycyclic aromatic hydrocarbons to marine organisms: a case study on the acute toxicity of pyrene to the European seabass (Dicentrarchus labrax L.), *Chemosphere*, 2012, **86**(9), 926–937.
3 W. Wang, M. J. Huang, Y. Kang, H. S. Wang, A. O. Leung, K. C. Cheung and M. H. Wong, Polycyclic aromatic hydrocarbons (PAHs) in urban surface dust of Guangzhou, China: status, sources and human health risk assessmen, *Sci. Total Environ.*, 2011, **409**(21), 4519–4527.
4 C. Rav-Acha and M. Rebhun, Binding of organic solutes to dissolved humic substances and its effects on adsorption and transport in the aquatic environment, *Water Res.*, 1992, **26**(12), 1645–1654.
5 L. Tremblay, S. D. Kohl, J. A. Rice and J. P. Gagné, Effects of temperature, salinity, and dissolved humic substances on the sorption of polycyclic aromatic hydrocarbons to estuarine particles, *Mar. Chem.*, 2005, **96**(1), 21–34.
6 B. Raber, I. Kögel-Knabner, C. Stein and D. Klem, Partitioning of polycyclic aromatic hydrocarbons to dissolved organic matter from different soils, *Chemosphere*, 1998, **36**(1), 79–97.
7 T. D. Gauthier, E. C. Shane, W. F. Guerin, W. R. Seitz and C. L. Grant, Fluorescence quenching method for determining equilibrium constants for polycyclic aromatic hydrocarbons binding to dissolved humic materials, *Environ. Sci. Technol.*, 1986, **20**(11), 1162–1166.
8 K. M. Danielsen, Y. P. Chin, J. S. Buterbaugh, T. L. Gustafson and S. J. Traina, Solubility enhancement and fluorescence quenching of pyrene by humic substances: The effect of dissolved oxygen on quenching processes, *Environ. Sci. Technol.*, 1995, **29**(8), 2162–2165.
9 M. A. Schlautman and J. J. Morgan, Effects of aqueous chemistry on the binding of polycyclic aromatic hydrocarbons by dissolved humic materials, *Environ. Sci. Technol.*, 1993, **27**(5), 961–969.
10 T. D. Gauthier, W. R. Seitz and C. L. Grant, Effects of structural and compositional variations of dissolved humic materials on pyrene Koc values, *Environ. Sci. Technol.*, 1987, **21**, 243–248.
11 M. U. Kumke, H. G. Löhmannsröben and T. Roch, Fluorescence quenching of polycyclic aromatic compounds by humic acid, *Analyst*, 1994, **119**, 997–1001.
12 F. D. Kopinke, A. Georgi and K. Mackenzie, Sorption and chemical reactions of PAHs with dissolved humic substances and related model polymers, *Acta Hydrochim. Hydrobiol.*, 2001, **28**, 385–399.
13 D. A. Backhus, C. Golini and E. Castellanos, Evaluation of fluorescence quenching for assessing the importance of interactions between nonpolar organic pollutants and dissolved organic matter, *Environ. Sci. Technol.*, 2003, **37**, 4717–4723.
14 R. D. Holbrook, N. G. Love and J. T. Novak, Investigation of sorption behavior between pyrene and colloidal organic carbon from activated sludge processes, *Environ. Sci. Technol.*, 2004, **38**, 4987–4994.
15 R. von Wandruszka, The micellar model of humic acid: evidence from pyrene fluorescence measurements, *Soil Sci.*, 1998, **163**, 921–930.
16 V. A. Ganaye, K. Keiding, T. M. Vogel, M. L. Viriot and J. C. Block, Evaluation of soil organic matter polarity by pyrene fluorescence spectrum variations, *Environ. Sci. Technol.*, 1997, **31**, 2701–2706.
17 M. U. Kumke, F. H. Frimmel, F. Ariese and C. Gooijer, Fluorescence of humic acids (HA) and pyrene-HA complexes at ultralow temperature, *Environ. Sci. Technol.*, 2000, **34**, 3818–3823.
18 C. Young and R. von Wandruszka, A comparison of aggregation behavior in aqueous humic acids, *Geochem. Transact.*, 2001, **2**, 16.
19 M. M. D. Sierra, T. G. Rauen, L. Tormen, N. A. Debacher and E. J. Soriano-Sierra, Evidence from surface tension and fluorescence data of a pyrene-assisted micelle-like assemblage of humic substances, *Water Res.*, 2005, **39**, 3811–3818.
20 K. Nakashima, M. Maki, F. Ishikawa, T. Yoshikawa, Y. K. Gong and T. Miyajima, Fluorescence studies on binding of pyrene and its derivatives to humic acid, *Spectrochim. Acta, Part A*, 2007, **67**, 930–935.
21 V. Kazpard, B. S. Lartiges, C. Frochot, J. D. E. de la Caillerie, M. L. Viriot, J. M. Portal and J. L. Bersillon, Fate of coagu-

lant species and conformational effects during the aggregation of a model of a humic substance with Al 13 polycations, *Water Res.*, 2006, **40**, 1965–1974.

22 J. M. Siéliéchi, B. S. Lartiges, G. J. Kayem, S. Hupont, C. Frochot, J. Thieme and L. J. Michot, Changes in humic acid conformation during coagulation with ferric chloride: Implications for drinking water treatment, *Water Res.*, 2008, **42**, 2111–2123.

23 L. Wang, N. Liang, H. Li, Y. Yang, D. Zhang, S. Liao and B. Pan, Quantifying the dynamic fluorescence quenching of phenanthrene and ofloxacin by dissolved humic acids, *Environ. Pollut.*, 2015, **196**, 379–385.

24 H. M. Marwani, M. Lowry, B. Xing, I. M. Warner and R. L. Cook, Frequency-domain fluorescence lifetime measurements via frequency segmentation and recombination as applied to pyrene with dissolved humic materials, *J. Fluoresc.*, 2009, **19**, 41–51.

25 B. Pan, S. Ghosh and B. Xing, Nonideal binding between dissolved humic acids and polyaromatic hydrocarbons, *Environ. Sci. Technol.*, 2007, **41**(18), 6472–6478.

26 M. Keiluweit and M. Kleber, Molecular-level interactions in soils and sediments: the role of aromatic π-systems, *Environ. Sci. Technol.*, 2009, **43**, 3421–3429.

27 A. Y. Freidzon, R. R. Valiev and A. A. Berezhnoy, Ab initio simulation of pyrene spectra in water matrices, *RSC Adv.*, 2014, **4**, 42054–42065.

28 G. Herzberg, *Molecular spectra and molecular structure. Vol. 3. Electronic spectra and electronic structure of polyatomic molecules*, Van Nostrand, Reinhold, New York, 1966.

29 K. Kalyanasundaram and J. K. Thomas, Environmental effects on vibronic band intensities in pyrene monomer fluorescence and their application in studies of micellar systems, *J. Am. Chem. Soc.*, 1977, **99**, 2039–2044.

30 D. S. Karpovich and G. J. Blanchard, Relating the polarity-dependent fluorescence response of pyrene to vibronic coupling. Achieving a fundamental understanding of the py polarity scale, *J. Phys. Chem.*, 1995, **99**, 3951–3958.

31 M. Aschi, A. Fontana, E. M. D. Meo, C. Zazza and A. Amadei, Characterization of electronic properties in complex molecular systems: modeling of a micropolarity probe, *J. Phys. Chem. B*, 2010, **114**, 1915–1924.

32 G. B. Ray, I. Chakraborty and S. P. Moulik, Pyrene absorption can be a convenient method for probing critical micellar concentration (cmc) and indexing micellar polarity, *J. Colloid Interface Sci.*, 2006, **294**, 248–254.

33 A. Nakajima, Solvent effect on the vibrational structures of the fluorescence and absorption spectra of pyrene, *Bull. Chem. Soc. Jpn.*, 1971, **44**, 3272–3277.

34 A. K. Mukhopadhyay and S. Georghiou, Solvent-induced enhancement of weakly allowed vibronic transitions of aromatic hydrocarbons, *Photochem. Photobiol.*, 1980, **31**, 407–411.

35 I. V. Perminova and K. Hatfield, in *Use of humic substances to remediate polluted environments: from theory to practice*, ed. I. V. Perminova, K. Hatfield and N. Hertkorn, NATO Science Series: IV: Earth and Environmental Sciences, Springer, Dordrecht, The Netherlands, 2005, vol. 52, p. 3.

36 D. V. Kovalevskii, A. B. Permin, I. V. Perminova and V. S. Petrosyan, Conditions for acquiring quantitative 13C NMR spectra of humic substances. Moscow State University, *Vestn. Mosk. Univ.*, 2000, **41**, 39–42.

37 V. A. Kholodov, A. I. Konstantinov, A. V. Kudryvtsev and I. V. Perminova, Structure of Humic Acids in Zonal Soils from C-13 NMR Data, *Eurasian Soil Sci.*, 2011, **44**, 976–983.

38 I. V. Perminova, N. Y. Grechishcheva and V. S. Petrosyan, Relationships between structure and binding affinity of humic substances for polycyclic aromatic hydrocarbons: relevance of molecular descriptors, *Environ. Sci. Technol.*, 1999, **33**, 3781–3787.

39 Y. P. Chin, G. R. Aiken and K. M. Danielsen, Binding of pyrene to aquatic and commercial humic substances: the role of molecular weight and aromaticity, *Environ. Sci. Technol.*, 1997, **31**, 1630–1635.

40 E. C. Shen, M. Price-Everett and T. Hanson, Fluorescence measurement of pyrene wall adsorption and pyrene association with humic acids: an experiment for physical chemistry or instrumental methods, *J. Chem. Educ.*, 2000, **77**, 1617–1618.